Adsorption Behavior of PS-PEO Diblock Copolymers on Silver and Alumina Surfaces: A Surface Plasmon Resonance Study

ALEXANDROS G. KOUTSIOUBAS, NIKOLAOS SPILIOPOULOS, DIMITRIOS L. ANASTASSOPOULOS, ALEXANDROS A. VRADIS, CHRIS TOPRAKCIOGLU, GEORGE D. PRIFTIS

Department of Physics, University of Patras, GR 26 500, Greece

Received 8 December 2005; revised 1 March 2006; accepted 1 March 2006
DOI: 10.1002/polb.20806
Published online in Wiley InterScience (www.interscience.wiley.com).

ABSTRACT: In this work, the adsorption behavior at the silver/toluene and alumina/toluene interface of polystyrene–polyethylene oxide (PS-PEO) diblock copolymers of various molecular weights was investigated by implementation of the surface plasmon resonance (SPR) technique. This was accomplished under a careful choice of experimental setup and the use of a suitable physical model for the interpretation of the experimental data. Comparison between polystyrene homopolymer and PS-PEO diblock copolymer adsorption measurements indicate that PS-PEO is anchored on the alumina surface via the PEO block, while on silver the copolymer is attached by various chain segments. The measured final adsorption amounts on alumina are typical of end-attached polymeric brush formation while the dynamics of the adsorption process present two clearly different evolution regimes. This work provides insight into the many advantages of the use of the SPR technique as a valuable tool for similar surface studies. © 2006 Wiley Periodicals, Inc. J Polym Sci Part B: Polym Phys 44: 1580–1591, 2006
Keywords: adsorption; block copolymers; kinetics; surface plasmons

INTRODUCTION

Surface plasmon resonance (SPR) Spectroscopy is an optical experimental technique that is currently gaining wide recognition as a valuable tool for surface studies. Under certain conditions, it may offer real-time, *in situ*, nondestructive analysis of dynamic surface events and thus is capable of determining rates of adsorption and desorption for a range of interfacial processes. In recent years, the SPR technique has been used for *in situ* adsorption studies of self-assembled monolayers (SAM),[1] polymer adsorption on metal or chemically altered surfaces,[2–6] and in many biological applications such as protein interactions, lipid bilayers, tissue engineering, cell adhesion on biomaterial surfaces, and antigen–antibody binding.[7]

In many of the above applications and especially the cases where SPR is used as a biosensor,[8] the experimental data have been interpreted in a semiqualitative or phenomenological manner. In this study, it is demonstrated that by a careful choice of experimental setup and with the use of a proper physical model, the SPR technique may accurately monitor copolymer adsorption phenomena with long-term stability and high-time resolution.

Recently, Stroeve et al.[9,10] have used the SPR technique to follow the kinetics of assembly of amphiphilic block copolymers on SAM modified gold surfaces. Block copolymers represent an interesting group of materials for applications such as stabilization and flocculation of colloidal particles,[11] lubrication, enhancement of biocom-

Correspondence to: A. A. Vradis (E-mail: vradis@physics.upatras.gr)

Journal of Polymer Science: Part B: Polymer Physics, Vol. 44, 1580–1591 (2006)

patibility of artificial implants, and generally the manipulation of surface properties for nano-technological uses. These applications are based on the fact that the behavior of copolymers near a solid interface is quite different from their behavior in the bulk solution because of the existence of entropic constraints concerning the copolymer chain conformations near a surface.[12]

Block copolymers tethered to a surface through one or more blocks may form extended layers that are known as polymer brushes. In the case of A–B type diblock copolymer adsorption from selective solvents, one block (the "anchor") preferentially tethers onto the surface via physical interactions, allowing the other block ("buoy") to extend into solution in a "brush-like" conformation.[13–18] The characteristics of such self-assembled polymer brushes and their formation dynamics depend on the copolymer structure and size, the interactions between the blocks, the nature of the solvent and the surface, and so forth. The equilibrium properties of A–B type copolymer brushes are well understood and have been extensively studied by a variety of experimental techniques including surface force measurements[17–21] and neutron reflectometry.[21–24]

Various experimental techniques have been applied to study block copolymer adsorption kinetics, including ellipsometry,[25–32] quartz crystal microbalance,[33] attenuated total internal reflection infrared (Fourier transform infrared-ATR) spectroscopy,[34] reflectometry,[35,36] and the surface forces apparatus.[37] In this study, SPR spectroscopy is adopted to probe the kinetics and equilibrium properties of polystyrene–polyethylene oxide (PS-PEO) block copolymers at the toluene/alumina and toluene/silver interface. In comparison with some experimental techniques (e.g., quartz crystal microbalance), SPR has the advantage that no calibration problems are encountered while the physical characteristics of the surface plasmons strongly enhance the overall sensitivity.

Most SPR adsorption studies so far have involved plasmon excitation on silver or gold thin films. In this work, in addition to silver, surface plasmons are also excited on thin aluminum films while the copolymer adsorption is studied on the ultrathin naturally occurring oxide layer (alumina-Al_2O_3). This oxide layer is formed on the thin, freshly evaporated aluminum films because of aluminum's high reactivity toward atmospheric oxygen upon contact with air. It should be mentioned that aluminum surfaces and their coatings are very important in industrial applications since aluminum and its alloys are widely used in many areas of interest.

The experimental results presented here include the first *in situ* SPR adsorption kinetics measurements of five different PS-PEO block copolymers from nonmicellar toluene solutions on silver and alumina surfaces. The results are directly compared with theoretical predictions concerning the various qualitative stages of the adsorption process and with previous studies involving PS-PEO adsorption at different surfaces. Moreover, *ex situ* SPR measurements have been carried out on the formed copolymer layers to check the consistency of the adopted experimental method and the stability of the adsorbed layer under solvent rinse.

EXPERIMENTAL

SPR Spectroscopy

Free electrons near a metal boundary can, under certain conditions, perform coherent oscillations which are called surface plasmons.[38] These oscillations are electromagnetic surface waves that propagate along the interface between a metal and its dielectric environment. Their frequency ω is related to their wavevector k_x by a dispersion relation $\omega(k_x)$[39]

$$k_x = \frac{\omega}{c}\left(\frac{\varepsilon_1\varepsilon_2}{\varepsilon_1+\varepsilon_2}\right)^{\frac{1}{2}} \quad (1)$$

where ε_1 is the complex dielectric constant of the metal, ε_2 the dielectric constant of the medium that surrounds the metal, and c the speed of light in vacuum.

Surface plasmons can be excited by light in the so-called Kretschmann configuration[40,41] using a metal-coated prism. In this case, the evanescent waves produced by total internal reflection of p-polarized light on the coated face of the prism are coupled with the surface charges and when the projection of their wavevector parallel to the prism face k_x fulfils the dispersion relation (eq. 1), the surfaces charges oscillate collectively with a frequency ω.

For a surface plasmon on a thin metal film, the relationship between frequency and wavelength of the wave is not only influenced by the dielectric constant and thickness of the metal film but also depends strongly on the dielectric constants of

the materials in the vicinity of the film surface. These facts render SPR spectroscopy a very sensitive tool for surface studies, like the adsorption of molecules on a metal surface.

From an experimental point of view, the adjustment of the k_x component of the evanescent wavevector is achieved by the rotation of the metal-coated prism at incidence angles above the critical angle for total internal reflection. For a certain incidence angle, k_x matches the surface plasmon wavevector and a sharp minimum in the measured reflectivity is observed. The angular variation of the reflectivity will be called hereafter "reflectivity curve" (Fig. 1). Our effort in all experiments concerns the monitoring of the modifications (shift and broadening) in the reflectivity curve due to the changes in the dielectric environment of the metal.

One important requirement for the optical excitation of surface plasmons is that the electrons of the metal film should exhibit a gas-like behavior. So there are only a few candidates for optical excitation of surface plasmons like silver, gold, and aluminum. The characteristics of the reflectivity curve strongly depend on the complex dielectric constant of the metal. For example, in Figure 1, two experimental reflectivity curves are plotted. The first one that is characterized by a sharper minimum in the measured reflectivity corresponds to a 50 nm silver film, while the second curve corresponds to a 20 nm aluminum film. Aluminum has a bigger real and imaginary part of the dielectric constant in comparison to silver, leading to a quite wider reflectivity curve and to a less sharp drop in reflectivity.

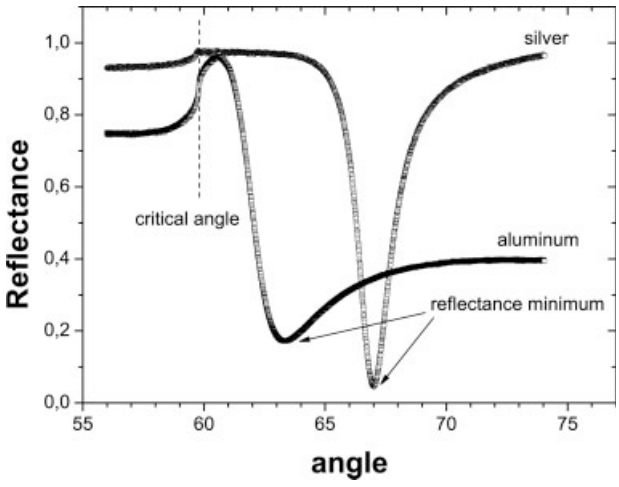

Figure 1. Typical experimental reflectivity curves for a 50 nm silver film and a 20 nm aluminum film in contact with toluene. The error of the measurement is smaller than the size of the experimental points in the graph.

Furthermore, the natural formation of a 2–3 nm aluminum oxide (Al_2O_3) layer on the aluminum surface induces a small shift of the reflectivity curve toward higher angles of incidence. This oxide layer is formed when freshly prepared aluminum films are exposed to atmospheric oxygen while it protects the film from further oxidation. Our preliminary test experiments confirmed that after its formation, this oxide layer is perfectly stable in contact with air and toluene.

SPR Apparatus

In this work, SPR spectroscopy measurements are performed in the Kretschmann configuration. The apparatus consists of a horizontal $\theta/2\theta$ goniometer based on two motorized, high precision rotators mounted one on top of the other with a common axis of rotation (Fig. 2). The lower rotator controls the angular position of the rotating sample stage with reference to the light beam. This rotation permits the continuous variation of incidence angle in a range of angles corresponding to k_x values around the value that fulfills the dispersion relation (eq. 1). The upper rotator is equipped with a custom-built aluminum arm on which the light detector is attached. The movement of this rotator is programmed in a way that ensures that the detector is always in the reflected beam ($\theta/2\theta$ movement). Both rotators have a precision in their movement, which permits an angular resolution of 0.01°.

A He-Ne laser beam ($\lambda = 632.8$ nm) is used as a light source for the excitation of surface plasmons. A beam splitter and a polarizer are placed between the light source and the sample in the primary beam path. The beam splitter is used for the formation of a secondary beam, which is recorded by a second photodiode to monitor and normalize the source light intensity. The polarizer is used for the *p*-polarization of the beam since surface plasmons are excited only by the *p*-component of electromagnetic waves, parallel to the metal surface. Both photodiode signals are measured simultaneously using two digital GPIB controlled A/D devices with external triggering. This configuration allows the normalization of the laser intensity and the suppression of the measured noise below 0.2% of the signal.

For the Kretschmann configuration, a silver or aluminum-coated optically flat equilateral SF10

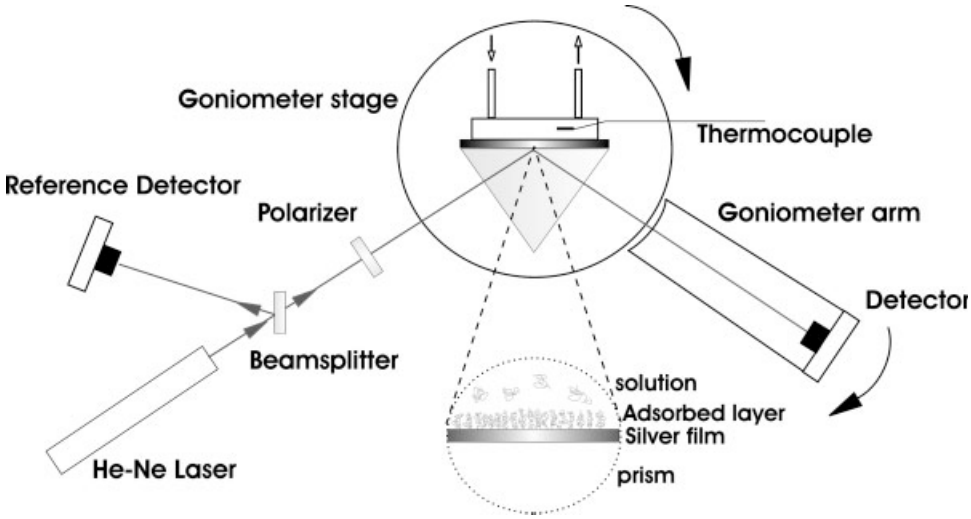

Figure 2. Representation of the SPR apparatus used in this study. The two detectors, thermocouple, and rotation motors are connected to and controlled by a digital computer. The magnified picture at the bottom illustrates the several layers that surround the thin metal film in the case of adsorption on silver.

prism ($n = 1.7230$) is used. Sample solution is placed in a custom built PTFE cell (15 mL capacity) which is sealed with the aid of a PTFE O-ring and by pressing the cell against the face of the prism. The temperature of the solution is monitored by a Teflon-coated thermocouple immersed in the solution.

The apparatus is fully computer controlled, while data acquisition software is custom developed in C language. The overall speed of the experimental setup permitted a reflectivity scan with 0.01° step over 2° every 6 s. For a full reflectivity scan over 20° (Fig. 1), the time needed exceeds 1 min. However, test experiments proved that scanning 2° around the reflectance minimum provides adequate accuracy and time resolution for the monitoring of copolymer adsorption kinetics.

Sample Preparation

Sample preparation started by careful cleaning of the prism surfaces and all components that come into contact with the solution. The cleaning procedure that is adopted involves 24 h exposure to fresh sulfochromic acid, rinsing with deionized water, followed by 15-min ultrasonic bath in distilled water, rinsing with ethanol (AR quality) and finally drying in a stream of dry nitrogen. An aluminum film of about 20 nm and 99.999% purity or a silver film of about 50 nm and 99.999% purity is evaporated on the prism surface by thermal evaporation under a base pressure of about 1×10^{-6} Torr at a relatively slow rate (0.15 nm/sec), monitored by an oscillating quartz crystal. After the evaporation procedure, the system is kept in vacuum for half an hour and then the prism is removed from the evaporation chamber.

Experimental Procedure

Two homopolymers of polystryrene (purchased from Toyo Soda Manufacturing Co. Ltd) and five diblock copolymers of polystyrene (PS) poly-ethylene-oxide (PEO) (purchased from Polymer Laboratories) were used in this study. Their molecular weight, PEO content, and other characteristics are summarized in Table 1. Copolymer solution concentrations used during SPR experiments were in the range of 0.01–0.1 mg/mL. Under these conditions, no micelle formation is expected, as in dynamic light scattering experiments no micelles have been observed for similar solutions up to a concentration of 5.0 mg/mL.[25] All prepared solutions were allowed to equilibrate for about 12 h.

To achieve maximum accuracy, variations of temperature in the PTFE cell are monitored (± 0.1 °C precision) during adsorption experiments and temperature-corrected refractive indices are used in all calculations. It must be pointed out that in the absence of temperature correction, even small changes of the solution temperature may give rise to significant errors in the obtained results. For example, a temperature change of ΔT

Table 1. Characterization of Polymers Used in This Study

Polymer	Molecular Weight (M_w)	PEO Content wt %	Polydispersity (M_w/M_n)
PS 16.7K	16,700	0	1.02
PS 750K	750,000	0	1.01
PS-PEO 80K	80,000	5.0	1.07
PS-PEO 147K	147,000	1.3	1.09
PS-PEO 182.7K	182,700	4.2	1.07
PS-PEO 322K	322,000	2.4	1.19
PS-PEO 496.7K	496,700	1.2	1.18

$= 0.1$ °C would produce a systematic error of $\Delta\Gamma = 0.07$ mg/m^2 on the measured adsorbed amount. Using the SPR apparatus, the refractive index temperature gradient of toluene was measured by collecting reflectivity curves at various temperatures around 20 °C. The measured temperature gradient was found to be $(dn/dT = -5.0 \times 10^{-4}/°C)$, which is in excellent agreement with other reported experimental values.[42]

The first step in the experimental procedure is the optical alignment of the laser beam normal to the prism face, with an accuracy of $\pm 0.01°$. The angular variation of the reflectivity (reflectivity curve) of the metal film against air is recorded, leading to the determination of the thickness and complex dielectric constant of the film using a fitting procedure which is presented in the Data Analysis section. In addition, since the refractive indices of the prism and air are known very accurately, the measured position of the critical angle provides a cross-check of the laser beam alignment. Then the cell is filled with toluene (AR quality) and the reflectivity curve is recorded again. The thicknesses and dielectric constants of the alumimum and silver films were determined in contact with air (empty cell) and in contact with toluene. The average dielectric constant found was $\varepsilon_{Ag} = -17.6 + i0.70$ for silver and $\varepsilon_{Al} = -49.8 + i19.7$ for aluminum, in very good agreement with values quoted in the literature.[41] The determined thickness of each film and the thickness measured using the quartz crystal during evaporation were in agreement to within 5%.

In order to measure the polymer adsorption, the PS-PEO copolymer was dissolved in toluene and then injected to pure solvent in the cell. In this way, it is possible to achieve the desired concentration in the range 0.01–0.1 mg/mL. At the beginning of the adsorption process, the kinetics were followed by fixing the detector at a given angle, typically 1–2° less than the angle of the reflectance minimum, and the reflected light intensity was monitored as a function of time for about 1 or 2 min. Changes in light intensity are then related to the curve shift via the fitting procedure described below. This procedure permitted the acquisition of time-resolved information about the initial stages of the adsorption process with a sampling time of 1 s. After that the apparatus was programmed to scan continuously 2–4° around the reflectance minimum for about 120 min and then as the adsorption process slows down the system was switched to wider scans, covering 20° (Fig. 1). At the end of the adsorption phenomenon, the polymer-coated film surface is rinsed with toluene, dried, and measured in air (dry layer measurement). This procedure provides an independent measurement of the total adsorbed amount which is directly compared with the *in situ* measurements. Moreover, in this way, the stability of the adsorbed layer against solvent rinse is revealed.

Data Analysis

Adsorption on the metal or oxide surface induces a shift in the reflectance minimum toward higher angles and a slight broadening of the reflectivity curve since the index of refraction of the PS-PEO copolymer is higher than that of toluene [Fig. 3(a)]. It should be mentioned that the magnitude of these changes depends on the difference between solvent/polymer refractive indices, which in our case is relatively small ($\Delta n = n_{polystyrene} - n_{toluene} = 0.09$). In all calculations, the PS-PEO refractive index is set equal to the refractive index of PS ($n = 1.582$, $\lambda = 632.8$ nm) since the PS block of all used copolymers is much larger than the PEO block.

For the analysis of the experimental results, the reflectivity curves were fitted to a five-layer model as (prism/metal/oxide layer/adsorbed layer/solution) for *in situ* adsorption measurements,

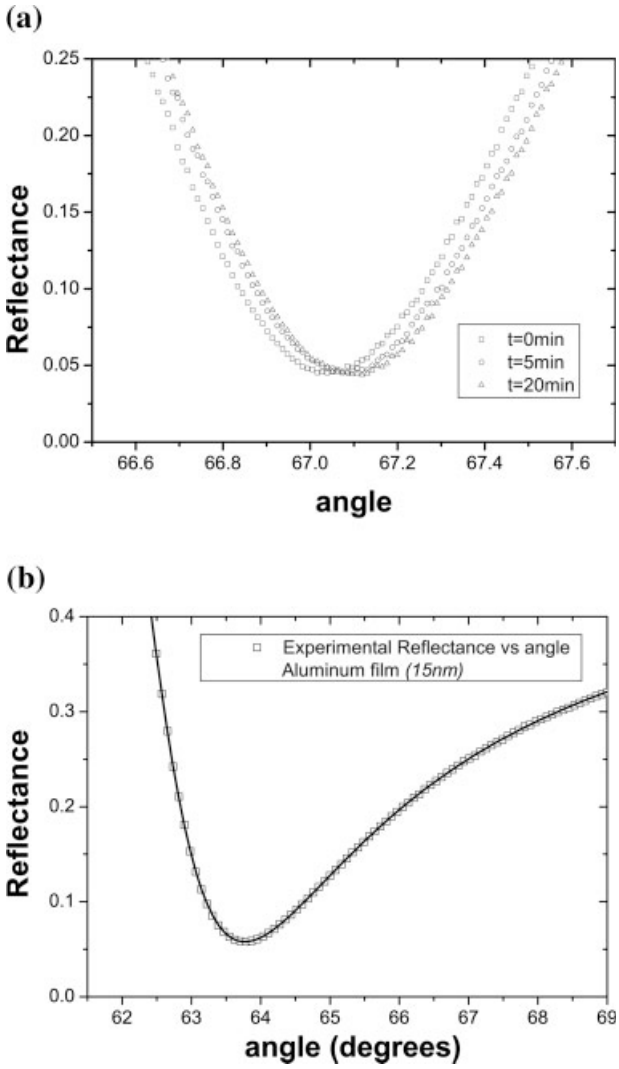

Figure 3. (a). Experimental SPR curves near reflectance minimum at different times for a silver film in contact with a 0.01 mg/mL PS-PEO 80K solution. The curve shift is indicative of the increasing copolymer concentration near the surface. (b). Typical experimental aluminum film SPR curve near the reflectance minimum. The continuous curve passing thought experimental points represent the result of the fitting procedure described in text. Not all experimental points are plotted for reasons of clarity.

and (prism/metal/oxide layer/copolymer/air) in the case of dry layer measurement. When silver films are used, the oxide layer is omitted from calculations. Initially, the fitting procedure concerns the determination of the complex dielectric constants and thicknesses of the metal and oxide films against air and toluene. The best fit [Fig. 3(b)] determines the following parameters of the metal film: the thickness, the real and imaginary part of the dielectric constant, and, additionally, when aluminum films are present, the parameters of the oxide layer: the thickness and the real part of the dielectric constant.

These values were then kept fixed for the fitting procedure of the reflectivity curves that were acquired during *in situ* adsorption measurements, while the refractive index of toluene was set according to the measured temperature. All experimental data were analyzed using the matrix formalism[43] for homogeneous stratified dielectric media and assuming that the refractive index of the copolymer layer near the surface is linearly dependent on the copolymer concentration, which is valid for low concentrations.[1] The dielectric constant of the adsorbed layer is approximated as $\varepsilon = V_s\varepsilon_s + V_p\varepsilon_p$, where ε_s and ε_p are the dielectric constants of solvent (toluene) and copolymer, respectively, while V_s and V_p are the fractional volumes occupied by the solvent and the polymer, respectively, in this layer ($V_s + V_p = 1$).

The fifth layer of the fitting model in the case of *in situ* measurements is the solution injected in the cell and considered as a semi-infinite layer. Despite the fact that all solutions used during the present adsorption studies are dilute, their refractive index change associated with concentration is not negligible. Especially at higher bulk solution concentrations ($\geq$0.5 mg/mL), the reflectivity curve is not only affected by the copolymer adsorption on the surfaces, but also by the concentration of the bulk solution. This effect is taken into account in all calculations by properly setting the refractive index of the solution layer according to its concentration.

From the reflectivity curve fitting of the adsorption data, two parameters were determined: the average thickness and concentration of the adsorbed layer. Although a separate determination of these two parameters is difficult for such dilute layers, their product is invariant. Determination of this product results in an unambiguous value of the adsorbed mass per surface area that is plotted against time, giving a kinetics curve. Under these conditions, the overall experimental error in the adsorbed mass was found to be less than ± 0.1 mg m^{-2}. All fitting algorithms used were developed in Fortran language, implementing the nonlinear Levenberg–Marquart least squares fitting method.[44]

RESULTS AND DISCUSSION

In this section, results concerning PS-PEO copolymer and PS homopolymer adsorption on silver

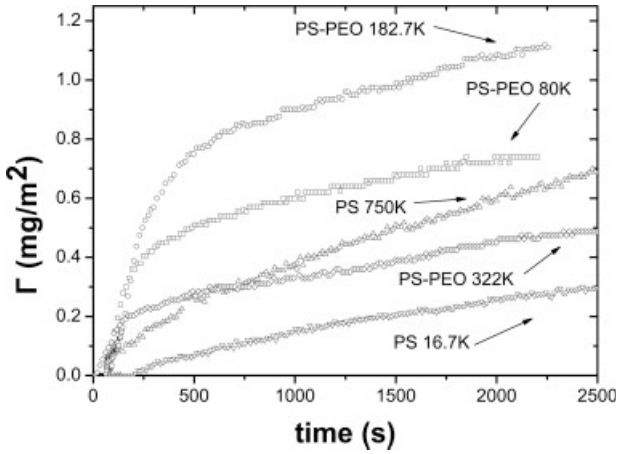

Figure 4. Adsorbed amounts on silver of PS-PEO 80K, PS-PEO 182.7K, PS-PEO 322K copolymers and PS 16.7K, PS 750K hopolymers as a function of adsorption time, as revealed from SPR measurements. The solution concentration is 0.01 mg/mL. All adsorption curves reach a plateau about 8 h after the initiation of the experiment. The final adsorbed amounts measured after 24 h are PS 750K (2.0 mg/m^2), PS-PEO 322K (2.0 mg/m^2), PS-PEO 182.7K (1.8 mg/m^2), PS-PEO 80K (1.1 mg/m^2), and PS 16.7K (0.8 mg/m^2).

and alumina surfaces are discussed. Figure 3(a) shows typical experimental silver film reflectivity curves near the reflectance minimum at different time intervals, after the injection of 0.1 mg/mL PS-PEO 80K solution into the PTFE cell, revealing some of the qualitative features of the adsorption runs.

Initially, we considered the adsorption behavior of PS-PEO diblock copolymers on silver surfaces. In Figure 4, representative adsorption kinetics curves for the adsorption on silver of PS 16.7K, PS 750K, and three PS-PEO copolymers at a bulk solution concentration of 0.1 mg/mL are presented. The observed copolymer adsorption rates do not seem to have any specific trend related to the molecular weight of the chains and were found to be quite low even at high bulk solution concentrations (80% of the final coverage is achieved after 2 h, and a final plateau is observed after ca. 8 h).

The copolymer kinetics on silver are not characterized by two distinct kinetic steps[25] while adsorption rate factors are about three orders of magnitude lower than those that have been measured for copolymer adsorption on silicon oxide surfaces. In the very early stages of the application of the SPR technique in adsorption studies, Loulergue et al.[45] have measured the adsorption of PS from toluene solutions on silver gratings. In agreement with the present findings, their results are characterized by relatively slow adsorption rates even for quite high solution concentrations as 10 mg/mL.

Furthermore, the measured final adsorbed amounts are lower than those that have been found on other surfaces like quartz and mica. As can be seen in Figure 4, the presence of a PEO block on the polymer chain does not significantly affect the adsorption phenomenon, since PS and PS-PEO solutions of the same concentration produce a comparable coverage, except for the low molecular weight PS 16.7K homopolymer. So we may conclude that in the case of a silver surface the adsorption energy parameters χ_s relative to the solvent toluene for the two blocks (PS and PEO) do not differ significantly. The general trend in the experimental data illustrates that longer chains tend to produce higher coverages on the silver surface, which is typical of homopolymer adsorption from good solvents[12] where chains are adsorbed by many chain segments.

On the contrary, all other PS-PEO adsorption runs conducted on alumina surfaces (Figs. 5 and 6), even at low bulk concentrations, (0.01 mg/mL) produced a surface coverage greater than 2.2 mg m^{-2}, while all PS 16.7K and PS 750K adsorption runs resulted at best in a surface coverage of 0.5 mg m^{-2}. In addition, the presence of a PEO block in the polymer chain fully enhances the measured adsorption rate on alumina surfaces.

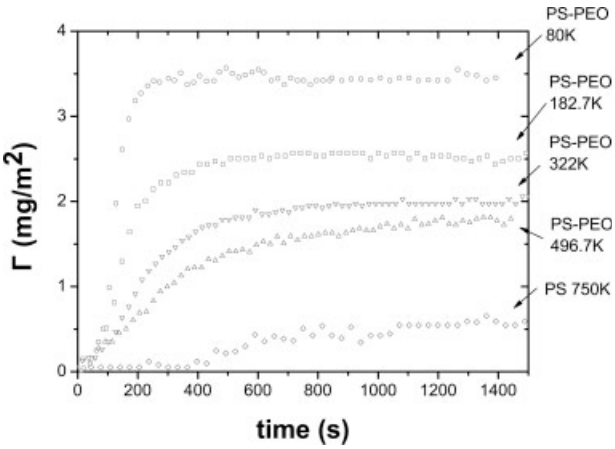

Figure 5. Adsorbed amounts on alumina of four different PS-PEO copolymers and two PS homopolymers as a function of time for 0.1 mg/mL bulk solution concentration. Each curve refers to the kinetics of a different copolymer or homopolymer that is noted on the right.

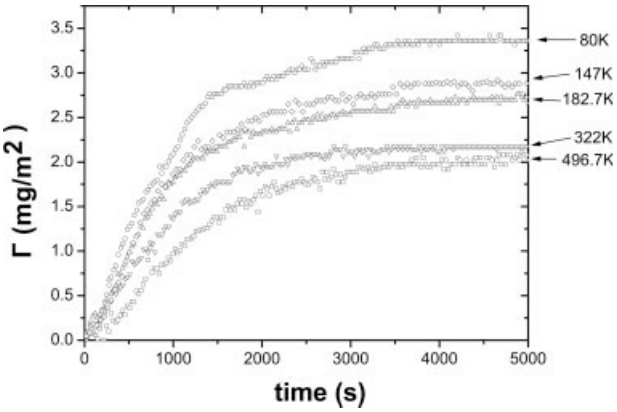

Figure 6. Adsorbed amounts on alumina of five different PS-PEO copolymers as a function of time for 0.01 mg/mL bulk solution concentration. Each curve refers to the kinetics of a different copolymer that is noted on the right.

These findings indicate the critical role of the PEO block in the adsorption process and lead to the conclusion that the PS-PEO copolymer is anchored to the alumina surface mainly via the PEO block. This same behavior is well established in other studies[22,25] for the toluene/silicon oxide interface, where it is shown that the adsorbed copolymer forms an extended brush. In the following sections, the adsorption kinetics and equilibrium properties of PS-PEO copolymers on alumina are discussed in detail.

Adsorption Kinetics

Adsorption kinetics data on alumina using the SPR technique were collected at room temperature (24–26 °C) for five PS-PEO diblock copolymers and two PS homolymers (Table 1), for two different bulk solution concentrations and are summarized in Figures 5 and 6, where the adsorbed amount per unit area is plotted against time.

It is evident that the amount of the adsorbed copolymer increases monotonically with time, while more than 80% of the final adsorption coverage is achieved within 10 min in the case of 0.1 mg/mL concentration, and within 45 min in the case of 0.01 mg/mL concentration. The adsorption of the two homopolymers proceeds with an obviously slower rate. No overshoot phenomena[26] have been observed. The slow adsorption up to 1 min can be attributed to the initial loading of the concentrated solution to the solvent. After that the adsorption proceeds at a faster rate.

A preliminary analysis showed that it is impossible to fit the entire adsorption kinetics curve to a simple model. This fact is not surprising since copolymer adsorption is a complicated process and is expected to have more than one stages. In the initial stage of the phenomenon, the alumina surface is totally uncovered and available for accommodating the incoming molecules. Theoretically under these conditions and until a certain coverage is reached, the adsorption is governed by a Fickian law (diffusion-controlled regime), which states that the adsorbed amount has a linear relation with the square root of the time.[25,27–29] This can be shown by solving the diffusion equation,

$$\frac{\partial c(z,t)}{\partial t} = D\frac{\partial^2 c(z,t)}{\partial z^2} \tag{2}$$

where t is time, c is the concentration, z denotes the direction normal to the surface, and D the diffusion coeffhcient of the copolymer in solution. Assuming that the alumina surface acts as a perfect sink (i.e., every molecule that reaches the surface is immediately attached) and that the solution has a homogeneous concentration, we may impose the following boundary conditions:

$$c(z=0,t)=0 \quad \text{and} \quad c(z,t=0)=c_0 \tag{3}$$

Where c_0 is the solution concentration. Then the adsorbed amount may be derived by the relation

$$\Gamma(t) = \int_0^t j(z=0,\tau)d\tau \tag{4}$$

where j is the flux to the surface that is determined by the derivative of the concentration profile. Combination of the above equations leads to the expression

$$\Gamma(t) = \frac{2}{\sqrt{\pi}}c_0\sqrt{Dt} \tag{5}$$

In Figure 7, the adsorbed amount as a function of the square root of time is plotted for a short time interval from the beginning of adsorption, for all five copolymers from a bulk solution concentration of 0.01 mg/mL. In this time interval, the initial linear relation is clearly observed.

In the current regime, it is possible to determine the diffusion coefficient D of the PS-PEO copolymer in toluene from the slope of the graph of the adsorbed amount versus the square root of

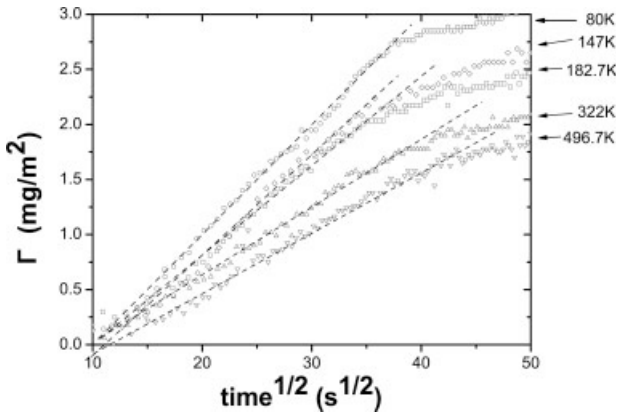

Figure 7. Adsorbed amounts on alumina of five different PS-PEO copolymers as a function of the square root of adsorption time for 0.01 mg/mL bulk solution concentration. The dashed lines indicate the fickian behavior at small times. Each curve refers to the kinetics of a different copolymer that is noted on the right.

time in eq. 5. For all measured solution concentrations, the diffusion coefficient obtained from such calculations is of the order 10^{-7} cm^2 s^{-1} as has been reported for the case of PS-PEO adsorption on the SiO_2/toluene interface.[25] Values of the diffusion coefficient for copolymers of similar molecular weight that have been measured by photon correlation spectroscopy are of the same order.

Dynamic scaling theory[46] predicts that the diffusion coefficient of a polymer chain in a good solvent scales according to the law $D \sim {M_w}^{-\nu_D}$, where $\nu_D = 0.588$. Dynamic light experiments give $\nu_D = 0.55 \pm 0.02$. The calculated values of the diffusion coefficients from the present experimental data are summarized in Table 2 and in Figure 8, where a plot of D versus M_w is presented.[47] From the slope of the line in Figure 8, we find a scaling exponent $\nu_D = 0.62 \pm 0.08$ which falls within previously reported theoretical and experimental results.

Beyond the diffusion-controlled regime, when a certain coverage $\tilde{\Gamma}$ is reached and the average distance between adsorbed chains becomes smaller, the preformed layer acts as a barrier for further molecules to reach the surface (brush-limited regime). This is the reason for the observed deviation from the initial Fickian behavior and for the significant decrease of the adsorption rate. Further adsorption involves chain deformation and rearrangement, which results essentially from a balance between the energy gain due to adsorption and the energy cost associated with chain stretching. Local rearrangement of already adsorbed chains to accommodate more incoming chains is clearly a slow process.

The increase of the adsorbed amount in this regime is expected to follow an exponential time dependence[25,27] that describes the slowing down of the adsorption process. The relation of the adsorbed amount versus time may be written as

$$\Gamma(t) = \Gamma_{max}(1 - e^{-kt}) + \tilde{\Gamma} \qquad (6)$$

where Γ_{max} is the final adsorbed amount and k the rate constant of this regime. Figure 9 shows the long time adsorption behavior of the lower and higher molecular weight copolymers for a concentration of 0.01 mg/mL, where the linear behavior after the initial fast process is indicative of the validity of eq. 6. The calculated values of the rate constants k for each copolymer range from 0.10 to 0.27 h^{-1} and are summarized in Table 2. In general, we observe that the rate constant k decreases with increasing molecular weight of the PS block. This trend is explained by

Table 2. Experimentally Determined Rate Factors and Equilibrium Characteristics of the Adsorbed Polymeric Layers on Alumina

PS-PEO copolymer M_w	D (10^{-7} cm^2/s)	k (hour^{-1})	Γ_{in} (mg/m^2)	Γ_{ex} (mg/m^2)	R_F (nm)	s (nm)	R_g (nm)	σ^*	R_F/s
80K	7.8	0.27	4.0	3.6	23.6	5.8	9.67	8.9	4.1
147K	6.2	0.18	3.5	3.5	33.7	8.3	13.89	8.7	4.0
182.7K	5.7	0.18	3.2	2.8	38.3	9.7	15.81	8.3	3.9
322K	3.2	0.11	2.9	2.8	53.4	13.6	22.15	8.3	3.9
496.7K	2.7	0.10	2.7	2.5	68.8	17.5	28.66	8.4	3.9

Diffusion coefficient D, brush-limited regime rate constant k, *in situ* final adsorbed amount Γ_{in}, *ex situ* final adsorbed amount Γ_{ex}, Flory radius R_F, spacing between the anchoring blocks s, radius of gyration R_g, reduced coverage σ^*, as calculated from SPR experiments on alumina at a 0.01 mg/mL bulk solution concentration.

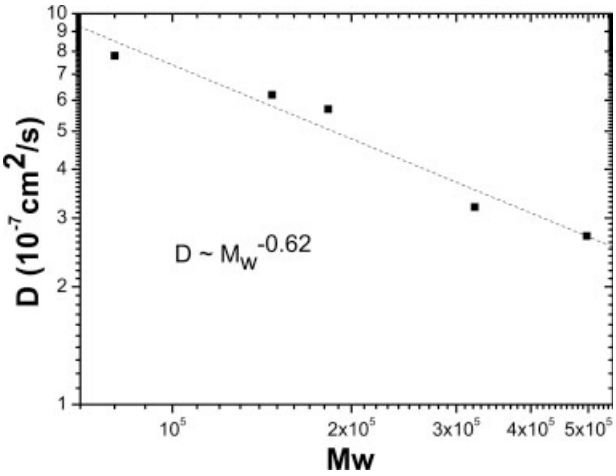

Figure 8. Plot of the diffusion coeficient versus copolymer molecular weight. The exponential factor of the power law is determined by a linear fit to the data.[47]

the fact that it is more difficult for longer chains to penetrate into the preformed polymeric layer, leading to an overall decrease in the adsorption rate.

These results support the picture that diblock copolymer adsorption from nonmicellar solutions is essentially a two-stage process on a clearly separated timescale. The initial diffusion-controlled regime lasts only for a relatively short period of time, giving its place to a much slower exponential process (brush-limited regime) until a plateau value for the adsorbed amount is reached, many hours later. In any case, within experimental error, no significant change was observed in the adsorption amount after 24 h. Test experiments at even higher time scales (3–4 days) supported the same conclusion.

Equilibrium Properties

All adsorbed amounts Γ_{in} that are presented in Table 2, were measured *in situ* 24 h after the initiation of the adsorption procedure. After each measurement, the alumina surface was rinsed with toluene and the collapsed copolymer layer was measured against air (dry layer measurement). These *ex situ* measurements gave copolymer adsorption masses Γ_{ex} that were consistent with the previous *in situ* measurements and their difference was found to be less than 15%. This means that no appreciable desorption occurs after the solvent rinse of the surface, which is indicative of the relatively strong attachment of the copolymer on the alumina surface.

The term "brush" is usually used in the literature when the mean distance between the anchoring blocks is significantly lower than the Flory radius of the polymer in solution. The Flory radius R_F of PS may be evaluated from[48] $R_F = 0.032\ M_w^{0.585}$ nm. The spacing between the PEO anchoring blocks is given by the expression[22]

$$s = \left(\frac{N_A \Gamma}{M_w}\right)^{-\frac{1}{2}} \tag{7}$$

where N_A is Avogadro's Number. We thus find that the spacing s for the studied copolymers ranges from about 5.8 to 17.5 nm (Table 2) while the ratio R_F/s ranges from 3.9 to 4.1. So for all studied copolymers, the Flory radius is about four times higher than the interanchor spacing, a ratio typical of a brush-like conformation for end-adsorbed chains, which is characterized by chain overlap and stretching.

Furthermore, by evaluating the radius of gyration of PS chains using $R_g = 0.0117\ M_w^{0.595}$ nm,[49] we have calculated the "reduced coverage" $\sigma^* = \pi R_g^2/s^2$, which is a ratio of the cross-sectional area of a free chain in solution to the average area per grafted chain. As seen in Table 2, the reduced

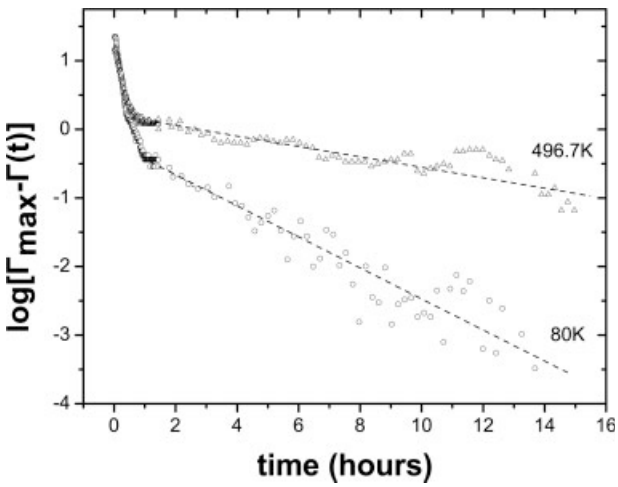

Figure 9. Long-time behavior of the adsorption for the 80K and 496.7K PS-PEO copolymers. The solution concentration is 0.01 mg/mL. Γ_{max} is the adsorbed amount at saturation (infinite time). In the initial stage, the diffusion-controlled regime is seen. At longer times, the linear behavior is indicative of the increase of the adsorbed amount according to an exponential law (eq. 6).

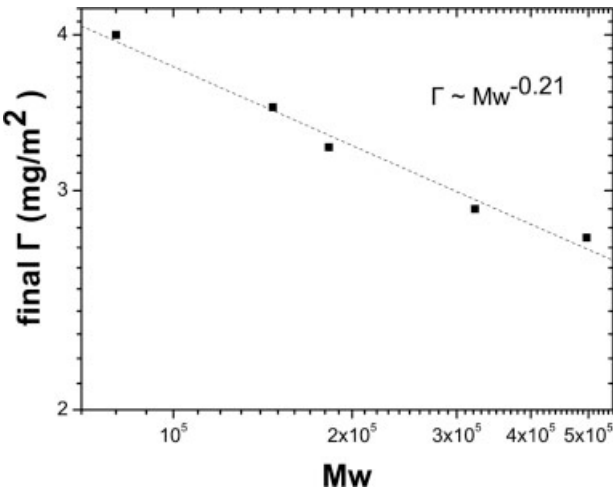

Figure 10. Plot of the final adsorbed amount versus copolymer molecular weight. The exponent of the power law is determined by a linear fit to the data.

coverage was found to reach values greater than 8, well beyond the onset of chain stretching.[49]

The final adsorbed amount presents a decrease as the molecular weight of the copolymer increases for both solution concentrations. A plot of the measured adsorption against copolymer molecular weight (Fig. 10) reveals a power law $\Gamma \sim M_w^{-\nu}$, where $\nu = 0.21 \pm 0.02$. In an ellipsometric study of PS-PEO adsorption from toluene solutions on a SiO_2 surface, where brush formation kinetics are discussed, Motschmann et al.[25] have found an exponent $\nu = 0.18$, which is very close to the present result. This result is in agreement with a simple scaling picture where the anchoring energy per chain is roughly equal for all diblock copolymers in our study. One would then expect that the number of "blobs," n_b, per chain would also be the same for all diblocks (this is because at equilibrium the anchoring energy per chain must be balanced by the osmotic repulsion per chain, which is of order kT per blob). This in turn implies that the brush height (given by the product of n_b with the blob size) is proportional to the blob size or the interanchor spacing, s. Since the brush height also scales with $Ns^{-2/3}$ while the adsorbance, Γ, is proportional to Ns^{-2}, it follows that Γ scales with $N^{-1/5}$.

CONCLUSIONS

In conclusion, our results demonstrate that SPR Spectroscopy is a promising technique for *in situ* monitoring of macromolecular adsorption on a solid metal or oxide surface. Under the adopted experimental conditions and data analysis scheme, the method is characterized by high accuracy, high-time resolution, and long-term stability. It is important to note that the SPR technique presents certain advantages over some other surface measurement techniques. In particular, (a) there is no need of chemical modification of the polymer structure to enhance measurement efficiency, (b) the technique is nondestructive, (c) measurements are performed easily *in situ* and *ex situ* on the same sample, (d) constant angle measurements fully enhance the overall time resolution, permitting the study of fast processes.

The presented results concern PS-PEO diblock copolymer adsorption on silver and alumina in the presence of a selective solvent (toluene). On the basis of the differences observed between PS and PS-PEO adsorption measurements, we conclude that the adsorbed PS-PEO copolymer is attached on silver not only by the PEO blocks but also by various PS chain segments while on alumina it is end-grafted via the PEO block leading to adsorbed amounts typical of a polymer brush formation.

The kinetic study on silver surfaces revealed that PS-PEO and PS adsorption proceeds with a comparable rate which is substantially lower than the observed rates of PS-PEO adsorption on alumina. When the copolymer is end-grafted by one block (as in the case of PS-PEO on alumina), the kinetics are characterized by two distinct time regimes governed by a Fickian and an exponential law respectively, in accordance with previous experimental observations. The overall observed adsorption rates on alumina are similar to adsorption rates of similar copolymers on other surfaces like quartz or glass. Very good agreement with theory and other experimental observations was found for the scaling behavior of the diffusion coefficient and the final adsorbed amount versus molecular weight.

For the first time, there is experimental evidence of PS-PEO self assembly on alumina surfaces related to polymeric brush formation. Further investigations using the SPR technique involving more complex systems will provide information about their adsorption mechanisms while they may serve as model applications for the use of the SPR technique as an analytical tool in a wide range of surface studies.

We would like to thank one of the reviewers for his supportive and helpful comments on the interpretation of our final adsorbed amount data.

REFERENCES AND NOTES

1. Peterlinz, K. A; Georgiadis, R. Langmuir 1995, 12, 4731–4740.
2. Green, R. J.; Tasker, S.; Davies, J.; Davies, M. C.; Roberts, C. J.; Tendler, S. J. B. Langmuir 1997, 13, 6510–6515.
3. Tassin, J. F.; Siemens, R. L.; Tang, W. T.; Hadziioannou, G.; Swalen, J. D.; Smith, B. J Phys Chem 1989, 93, 2106–2111.
4. Yu-Wen, H., Gupta, V. K. Macromolecules 2001, 34, 3757–3764.
5. Knoll, W. MRS Bull 1991, 16(7), 29–38.
6. Advicula, R.; Aust, E.; Meyer, W.; Knoll, W. Langmuir 1996, 12, 3536–3540.
7. Green, R. J.; Frazier, R. A.; Shakesheff, K. M.; Davies, M. C.; Roberts, C. J.; Tendler, S. J. B. Biomaterials 2000, 21, 1823–1835.
8. Rich, R. L.; Myszka, D. Z. J Mol Recognit 2003, 16, 351–382.
9. Brandani, P.; Stroeve, P. Macromolecules 2003, 36, 9492–9501.
10. Brandani, P.; Stroeve, P. Macromolecules 2003, 36, 9502–9509.
11. Napper, D. H. In Polymeric Stabilization of Colloidal Dispersions. Academic: London, 1983.
12. Fleer, G. J.; Cohen Stuart, M. A.; Scheutjens, J. M. H. M.; Cosgrove, T.; Vincent, B. In Polymers at Interfaces. Chapman & Hall: Bristol, 1993.
13. Taunton, H. J.; Toprakcioglu, C.; Fetters, L. J.; Klein, J. Nature 1988, 332, 712–714.
14. Alexander, S. J Phys 1977, 38, 983–987.
15. de Gennes, P. G. Macromolecules 1980, 13, 1069–1075.
16. Halperin, A.; Tirrell, M.; Lodge, T. P. Adv Polym Sci 1991, 100, 31–71.
17. Taunton, H. J.; Toprakcioglu, C.; Fetters, L. J.; Klein, J. Macromolecules 1990, 23, 571–580.
18. Hadziioannou, G.; Patel, S.; Granick, S.; Tirrell, M. J Am Chem Soc 1986, 108, 2869–2876.
19. Balastre, M.; Li, F.; Schorr, P.; Yang, J.; Mays, J. W.; Tirrell, M. V. Macromolecules 2002, 35, 9480–9486.
20. Belder, G. F.; Ten Brinke, G.; Hadjiioannou, G. Langmuir 1997, 13, 4102–4105.
21. Cosgrove, T.; Phipps, J. S.; Richardson, R. M.; Hair, M. L.; Guzonas D. A. Macromolecules 1993, 26, 4363–4367.
22. Field, J. B.; Toprakcioglu, C.; Ball, R. C.; Stanley, H. B.; Dai, L.; Barford, W.; Penfold, J.; Smith, G.; Hamilton, W. Macromolecules 1992, 25, 434–439.
23. Satija, S. K.; Majkrzak, C. F.; Russell, T. P.; Sinha, S. K.; Sirota, E. B.; Hughes, G. J. Macromolecules 1990, 23, 3860–3864.
24. Field, J. B.; Toprakcioglu, C.; Dai, L.; Hadziioannou, G.; Smith, G.; Hamilton, W. J Phys II 1992, 2, 2221–2235.
25. Motschmann, H.; Stamm, M.; Toprakcioglu, C. Macromolecules 1991, 24, 3681–3688.
26. Dorgan, J. R.; Stamm, M.; Toprakcioglu, C.; Jerome, R.; Fetters, L. J. Macromolecules 1993, 26, 5321–5330.
27. Amiel, C.; Sikka, M.; Schneider, J. W.; Yi-Hua T.; Tirrell, M.; Mays, J. W. Macromolecules 1995, 28, 3125–3134.
28. Siqueira, D. F.; Stamm, M.; Breiner, U.; Stadler, R. Polymer 1995, 36, 3229–3233.
29. Abraham, T. Polymer 2002, 43, 849–855.
30. Dorgan, J. R.; Stamm, M.; Toprakcioglu, C. Polymer 1994, 34, 1554–1557.
31. Toomey R.; Mays J.; Tirrell M. Macromolecules 2004, 37, 905–911.
32. Toomey R.; Mays J.; Wade Holley D.; Tirrell M. Macromolecules 2005, 38, 5137–5143.
33. Mi-Kyoung P; Ji Ho Y; Pispas, S.; Hadjichristidis, N.; Advincula, R. Langmuir 2002, 18, 8040–8044.
34. Gragson, D. E.; Manes, J. P.; Smythe, J. E.; Baker, S. M. Langmuir 2003, 19, 5031–5035.
35. Bijsterbosch, H. D.; Cohen Stuart, M. A.; Fleer, G. J. Macromolecules 1998, 31, 9281–9294.
36. Leermakers, F. A. M.; Gast, A. P. Macromolecules 1991, 24, 718–730.
37. Pelletier, E.; Stamouli, A.; Belder, G. G.; Hadziioannou, G. Langmuir 1997, 13, 1884–1886.
38. Ritchie, R. H. Phys Rev 1957, 106, 874–881.
39. Abeles, F. Surf Sci 1976, 56, 237–251.
40. Kretschmann, H.; Raether, H. Z Naturforsch 1968, 23a, 2135–2136.
41. Raether, H. Surface Plasmons on Smooth and Rough Surfaces and Gratings; Springer-Verlag: Hamburg, 1986.
42. El-Kashef, H. Rev Sci Instrum 1998, 69, 1243–1245.
43. Born, M.; Wolf, M. Principles of Optics; Pergamon Press: London, 1959.
44. Press, W. H.; Teukolsky, S. A.; Vetterling, W. T.; Flannery, B. P. In Numerical Recipes in Fortran: the art of scientific computing; Cambridge University Press: Cambridge, 1992.
45. Loulerge, J. C.; Levy, Y.; Allain, C. Macromolecules 1985, 18, 306–307.
46. de Gennes, P. G. Scaling Concepts in Polymer Physics; Cornell University Press: Paris, 1979.
47. The D values presented in Figure 8 were extracted from the 0.01 mg/ml data. This is because diffusion is slower at this lower concentration, and measurement of the initial stages of adsorption yields more reliable diffusion coefficients than in the high concentration case (0.1 mg/mL) where the experimental uncertainties at very small times are greater.
48. Roovers, J. E.; Toporowski, P. M. J Polym Sci Pol Phys 1980, 18, 1907–1917.
49. Kent, M. S.; Lee, L. T.; Farnoux, B.; Rondelez, F. Macromolecules 1992, 25, 6240–6247.